Out of the blue; Phototropins of the leaf vascular bundle sheath mediate the blue light regulation of the leaf hydraulic conductance

Yael Grunwald [*] Sanbon Chaka Gosa[*] Tanmayee Torne Nava Moran Menachem Moshelion[#]

The Robert H. Smith Institute of Plant Sciences and Genetics in Agriculture, The Robert H. Smith Faculty of Agriculture, Food and Environment, The Hebrew University of Jerusalem, Rehovot 76100, Israel

*Both authors contributed equally to this work

[#]Correspondence: menachem.moshelion@mail.huji.ac.il (M. Moshelion)

ABSTRACT

The leaf vascular bundle sheath cells (BSCs), which tightly envelop the leaf veins, constitute a selective dynamic barrier to water and solutes radially entering the mesophyll and play a major role in regulating the leaf radial hydraulic conductance (K_{leaf}). Recently, we showed that the BSCs' plasma membrane H^+-ATPase, AHA2, increases K_{leaf} by acidifying the xylem sap. Since BL reportedly increases K_{leaf} and we found the blue light (BL) receptor genes, *PHOT1* and *PHOT2* expressed in the Arabidopsis BSCs, we hypothesized that, similar to the guard cells (GCs) BL signal transduction pathway, the BSCs' PHOT1 and PHOT2 activate the BSCs' H^+-ATPase and thus regulate K_{leaf}. Indeed, under BL illumination, the K_{leaf} in the knockout mutant lines *phot1-5*, *phot2-1*, *phot1-5phot2-1* and *aha2-4* was lower than in WT. BSCs-directed complementation (using the SCR promoter) of *phot1-5* and *aha2-4* respectively by *PHOT1* and *AHA2*, restored the BL-induced K_{leaf} increase. BSCs-specific silencing of *PHOT1* or *PHOT2* (using the SCR promoter) abolished the BL-induced K_{leaf} increase. Xylem-fed PHOT inhibitor, tyrphostin 9, also abolished the BL-induced K_{leaf} increase in WT. Moreover, in WT plants, white light (WL) acidified the xylem sap compared to dark, but did not acidify the xylem sap of the *phot1-5* mutant. BSCs-specific complementation of *phot1-5* by SCR: PHOT1, restored the WL-induced xylem acidification. On a cellular level, BL hyperpolarized the BSCs, which was prevented by tyrphostin 9. In addition, the osmotic water permeability coefficient (P_f) of the BSCs was higher under WL treatment. Our results link the blue light control of water fluxes from the xylem to the mesophyll via the BSCs in the following model:

BL →BSCs' *PHOT*s activation →tyrosine phosphorylation→BSCs' H^{+-} ATPase activation →BSCs hyperpolarization, xylem acidification →P_f elevation → K_{leaf} increase. Thus, this study is the first to demonstrate an independent BL signal transduction pathway regulation of the vascular tissue.

INTRODUCTION

Light, the energy source for photosynthesis, has also evolved as a signal that regulates growth and development (Kronenberg and Kendrick, 1986; Briggs and Huala, 1999) as well as physiological traits such as stomatal conductance (g_S) (Hsiao et al., 1973; Zeiger and Helper, 1977; Karlsson, 1986; Kinoshita et al., 2001; Talbott et al., 2003; Van Ieperen et al., 2012) and leaf hydraulic conductance (K_{leaf}) (Voicu et al., 2008; Ben Baaziz et al., 2012; Aasamaa and Sõber, 2012; Prado and Maurel, 2013). One of the most conserved and well-studied light-sensing mechanisms is that of the blue light (BL, 390-550 nm)-which invokes stomatal opening (Grondin et al., 2015). In this signal transduction pathway, BL is perceived by the guard cells (GCs) light-activated protein kinases PHOT1 and PHOT2 (Briggs and Christie, 2002; Kinoshita et al., 2001), eventually activating the plasma membrane H^+-ATPases (Kinoshita and Shimazaki, 1999; Svennelid et al., 1999), which, in turn, hyperpolarizes the GCs and acidifies their surrounding apoplast (Ueno et al., 2005; Den Os et al., 2007; Elmore and Coaker, 2011; Kinoshita and Shimazaki, 1999), recently reviewed by Inoue & Kinoshita (2017). Consequently, the hyperpolarization-activated inward-rectifying K^+ channels (K_{in}) are gated open enabling potassium ions (K^+) influx driven by K^+ electrochemical potential difference. Inward K^+ fluxes result in an osmolyte accumulation reducing the water potential inside the cell, which, in turn, drives an influx of water leading to GCs swelling and stomatal opening (Assmann, 1993; Roelfsema and Hedrich, 2005; Shimazaki et al., 2007; Oishi et al., 2010; Yamauchi et al., 2016).

Conversely, at night, in the dark, the guard cells' H^+-ATPases are deactivated, they are depolarized and their apoplast is alkalized (Kinoshita et al., 2001; Kinoshita and Shimazaki, 1999).

Blue light or white light (WL) illumination has also been shown to increase the hydraulic conductance (K_{leaf}) of the entire leaf in several plant species (Voicu et al., 2008 (bur oak); Voicu et al., 2009; Sellin et al., 2011 (silver birch); Aasamaa and Sber, 2012 (deciduous trees); Ben Baaziz et al., 2012 (walnut)). Interestingly, K_{leaf} has shown a faster response to light than g_S (Guyot et al., 2012). However, the molecular mechanism of K_{leaf} induction by light is not yet fully understood.

In the past decade, it has been established that the bundle sheath cells (BSCs), a parenchymatous layer which tightly enwraps the entire leaf vasculature, can act as a dynamic and selective xylem-mesophyll barrier to water and ions, which participates in K_{leaf} regulation (Shapira et al., 2009; Shatil-Cohen and Moshelion, 2012; Sade et al., 2014; Wigoda et al., 2014, 2017; Grunwald et al., 2020). Moreover, we recently discovered that the BSCs' H^+-ATPase proton pump, AHA2, participated in regulating $K_{leaf,}$ via changes in the xylem pH and the positive correlation between AHA2-driven xylem acidification and K_{leaf} was due to an increase in the osmotic water permeability of the BSCs membrane (Grunwald et al., 2020). AHA2 was reported (Wigoda et al., 2017 GEO repository Experiment GSE85463) to have an over-three-fold higher expression level in the BSCs than in the neighboring mesophyll cells, explaining how such acidification is possible. In addition, the same BSC transcriptome analysis (ibid.) revealed that the BL receptors PHOT1 and PHOT2 were substantially expressed in the BSCs, as well as their immediate phosphorylation substrate, BLUS1 (Blue Light Signaling1, At4g14480; (Takemiya et al., 2013)) and the BLUS1-interacting kinase, BHP (Blue-light-dependent H^+-ATPase Phosphorylation, At4g18950), elements of early BL signaling in the guard cells (reviewed

by Inoue and Kinoshita, 2017). These findings led us to hypothesize that a BL signal transduction pathway similar to that active in opening stomata is active also in the vascular BSCs and that it has a role in the regulation of K_{leaf}.

In confirmation of this hypothesis, we describe here a few of the physiological and molecular details of the mechanism underlying the blue light-dependent K_{leaf} regulation by BSCs.

MATERIALS AND METHODS

Plant material

Plant types. We used WT (wild type) *Arabidopsis thaliana* plants ecotype Colombia, Col-0 (aka Col), the T-DNA insertion AHA2 mutants *aha2-4* (SALK_ 082786) (Col) and *aha2-4* complemented with *SCR: AHA2* (line 56) (Col), and *SCR:GFP* (Col) as described in (Grunwald et al., 2020). In addition, we used WT Arabidopsis (Col) with the Glabrous mutation (WT Col-gl), *phot1-5 (nph1-5)* (Col-gl), *phot 2-1(npl1-1 or cav1-1)* (Col-gl) and the double mutant *phot1-5phot2-1 (nph1-5 npl1-1)* (Col-gl) (Kagawa et al., 2001), which were kindly provided by the Ken-Ichiro Shimazaki lab (Tokyo, Japan,).

Construction of transgenic plant lines. *SCR:mirPHOT* Plants**:** The premiR-PHOT1or PHOT2 and synthetic genes were synthesized by Hylabs (Rehovot, Israel), based on a premiR164 backbone (Alvarez et al., 2006). We used the Web-based MicroRNA Designer (WMD, http://wmd3.weigelworld.org) to produce a premiRNA gene MIR319a as described in WMD. After sequence verification, the premiR-PHOT1or premiR-PHOT2 were cloned into the pDONR™ 221 and the SCR promoter into pDONRP4P1r (Invitrogen) vectors which are Gateway® compatible by BP reactions, and later cloned into the pB7M24GW (Invitrogen) two fragment binary vector by LR reaction according to the manufacturer's instructions. Each binary vector was transformed into Agrobacterium by electroporation and transformed to WT Col0 using the floral dip method (Clough and Bent,

1998). Transformants were selected based on their BASTA (Glufosinate Ammonium, Sigma cat # 45520) resistance, grown on plates with MS (Murashige and Skoog, Duchefa cat# M222.0050) Basal medium + 1 % sucrose and 20 µg/ml BASTA. DNA insertion was verified in selected lines by PCR targeting the junction of the premiR-gene and the 35S terminator with the forward primer located about 1000bp from the 3' end of premiR-gene and reverse primer on the 35S terminator (see primer list in supplemental Table S1), PCR fragments were then sequenced and verified.

SCR: PHOT1 plants. Binary vectors were constructed with the *PHOT1* gene as described above and then transformed into *phot1-5* (Col-gl1) plants, and successful transformation was verified by PCR.

Plant Growth Conditions. Plants were grown in soil (Klasmann686 Klasmann-Deilmann, Germany) + 4g/l Osmocote® 6M in a growth chamber at 22 °C and 70% relative humidity, and 8-h light/16-h dark photoperiod. During the day, the illumination, humidity and VPD changed in a pattern resembling natural conditions, as in (Negin and Moshelion, 2017). The illumination intensity provided by LED lights strips (EnerLED 24 V-5630, 24 W/m, 3000 K (50%)/6000 K (50%)) reached up to 150-200 µmol m^{-2} sec^{-1} light at the plant level. The plants were irrigated twice a week.

Detached leaves preparation for gas exchange measurements. Fully expanded leaves from 7-8- week-old plants were excised at the petiole base using a wet sharp blade under a drop of water. Petioles were immediately submerged in 0.5 ml Eppendorf tubes with artificial xylem solution (AXS; 3 mM KNO_3, 1 mM $Ca(NO_3)_2$, 1 mM $MgSO_4$, 3 mM $CaCl_2$, 0.25 mM NaH_2PO_4, 90 µM EDFS (Sigma). The leaves were excised, shortly before "lights OFF" transition (around 5:00 PM) on the evening preceding the measurements and placed in gas-sealed transparent 25 cm x 20 cm x 15 cm plastic boxes with water-soaked tissue paper on the bottom to provide ~90% humidity. The transparent boxes were then inserted

into a larger light-proof plastic box overnight and kept in total darkness until the start of light treatments in the next morning.

Light treatments of detached leaves

All gas exchange experiments were conducted in a dark room (<1 umol m^{-2} s^{-1}) at a constant temperature of 22 °C, in the morning between 10:00 AM and 1:00 PM. The excised leaves were taken out of the light-sealed box, and placed in one of two custom-made light chambers (either red light (RL) or combined red and blue light (RL+BL), as specified further down). Leaves were exposed to either RL or RL+BL for 15 minutes in ambient vapor pressure deficit (VPD) of 1.3-1.5. A fan circulated the air in each light chamber for uniform and constant temperature and VPD. Next, leaves were transferred to a Li-cor 6400XT for an additional 2-3 minutes, under the same illumination conditions with VPD of about 1.3, until stabilization of the gas exchange measurements, after which the measurement was recorded. The total illumination intensity in both light chambers was set to roughly 220 µmol m^{-2} s^{-1}. In the RL chamber the leaves were illuminated only with red light (660 nm) and in the 'RL+BL' chamber they were illuminated with approximately 90% red light and 10% blue light (450 nm). D-LED lighting with adjustable current source (DR-SD6/12) was used as light sources (http://www.d-led.net/). Light intensity was verified daily using a LI-250A light meter with a LI-190SA quantum sensor (LI-COR, Lincoln, NE, USA).

Determination of gas exchange, E , g_S, and hydraulic conductance, K_{leaf}

Immediately after the light treatments, the leaves were placed in a LI-COR 6400XT for measurements of g_S (stomatal conductance) and E (transpiration) similar to Grunwald et al., 2020, with the following changes: all the experiments were conducted in the dark room at 22 C^0 and the illumination in the LI-COR cuvette was adjusted to match the preceding

158 light treatments. Immediately thereafter, the water potential (Ψ_{leaf}) was determined in a
159 pressure chamber (ARIMAD-3000; MRC Israel) and K_{leaf} was calculated (as in Grunwald
160 et al., 2020). *Eq. 1:* $K_{leaf} = -E / (\boldsymbol{\Psi}_{leaf} - \boldsymbol{\Psi}_{AXS}) \approx -E / \boldsymbol{\Psi}_{leaf}$,

161 Additionally, g_s was measured at the same time as above using LI-COR 6400XT on intact
162 leaves of whole plants left under the growth-room illumination for 2-4 hours after Lights
163 ON. Illumination settings in the instrument's cuvette were set to the same conditions as in
164 the growth room.

165 **Inhibition of light transduction in detached leaves**

166 Tyrphostin 9 (ENZO, cat. # BML-EI21, 100 mM in DMSO (Sigma, cat # W387520), kept
167 in aliquots at -18 ^{o}C), was added to the AXS to a final concentration of 10 µM. AXS with
168 DMSO at a concentration of 100 µl/l (vol/vol) served as a control in this set of experiments.
169 Excised leaves were kept overnight until the measurements as described above. For surface
170 application, 0.05% of Tween 20 (J.T. Baker cat# X251-07) was added to the Tyrphostin 9
171 and control solutions and sprayed prior to overnight perfusion with unmodified AXS.
172 Boxes holding the sprayed leaves did not contain the damp tissue paper, and leaves were
173 patted dry prior to placing them in the light chamber to ensure the leaf surface is dry when
174 placed in LI-COR 6400xt cuvette.

175 **Determination of xylem sap pH in detached leaves**

176 ***Leaf preparation for imaging.*** On the eve of the experiment, leaves from 6-7 week old
177 plants, approximately 2.5 cm long and 1 cm wide, were excised with a sharp blade and
178 perfused (as described) with AXS containing 100 µM of the dual-excitation fluorescent pH
179 probe, FITC-D (fluorescein isothiocyanate conjugated to 10 kD dextran, (Sigma cat. #:
180 FD10S), added from a 10 mM stock in DDW). The excised leaves were then placed in the

"double box" setup (i.e. sealed plastic box inside a dark box) and kept in the dark until measurements the next morning.

Dark-treated leaves: Leaves were taken out of the dark boxes and immediately prepared for vein imaging on a microscope slide under low light conditions (<5 μmol m^{-2} sec^{-1}).

Light-treated leaves: Leaves were taken out of the dark boxes and placed in the growth chamber inside transparent gas sealed boxes (boxes as in K_{leaf}) for 30 minutes of growth room white light illumination (see above under "Plant growth conditions") and were subsequently imaged.

The leaves were imaged using an inverted microscope (Olympus-IX8, as detailed by Grunwald et al., 2020). Image capture and image analysis of the intra-xylem pH were as already described (ibid.).

Determination of the BSCs membrane potential

BSCs protoplasts imaging. For the evaluation of protoplast membrane potential, we used a fluorescent membrane-potential-sensitive dual-excitation ratiometric dye Di-8-ANEPPS (Pucihar et al., 2009) and an inverted epifluorescence microscope (Eclipse Ti-S, Nikon, Tokyo, Japan) coupled to an IXON Ultra 888 camera (Andor, UK). BSC protoplasts isolated (Shatil-Cohen et al., 2014) from 6-8 weeks old SCR:GFP (Col) plants were kept at room temperature in the dark. A sample with a few protoplasts was placed in a bath solution in an experimental chamber, containing 30 μM di-8-ANEPPS and 1% pluronic acid, without or with 10 μM tyrphostin 9 (see Solutions below), and allowed to settle for 10 min on a glass coverslip bottom. A Nikon 40X objective (Plan Fluor 40x/ 0.75, OFN25 DIC M/N2) was used for protoplast viewing and imaging. An individual, perfectly round BSC (25-32.5 μM diameter) was selected for further imaging based on its GFP fluorescence (excitation of 490/15 nm was delivered by a xenon lamp monochromator, Polychrome II

(Till Photonics, Munich, Germany), under the control of IW6.1 (Imaging Workbench 6.1) software (Indec Biosystems, Santa Clara, CA), and the emitted fluorescence was filtered via a 515 nm dichroic mirror and a 525/50 nm band-pass barrier filter).

Protoplasts light treatment and imaging. The selected BSC protoplast in the experimental chamber was then darkened for 10-20 min (Control), and a first pair of images of di-8-ANEPPS fluorescence was recorded (excitation by a pair of 50 ms pulses, 438 nm then 531 nm, 3 ms apart, was delivered by the Polychrome II; the emitted fluorescence was filtered via a dichroic mirror of 570 nm and 585/20 nm emission band-pass filter (Chroma Technology Corp., Bellows Falls, VT, USA)). Subsequently, the protoplast was illuminated for 5-10 min with either RL (660 nm, 220 µmol m^{-2} s^{-1}) or RL+BL (220 µmol m^{-2} s^{-1}, BL 450 nm, 10-15% of the total intensity) and a second pair of fluorescence images was recorded as above. The images were processed using FIJI (Abràmoff et al., 2004; Schindelin et al., 2012) to yield a pixel-by-pixel fluorescence ratio as described earlier (Wigoda et al., 2017).

Fluorescence ratio calibration. BSCs protoplasts incubated in di-8-ANEPPS as above were subjected to 5 s-long voltage pulses in the range of +17 to -223 mV using a patch-clamp pipette in a whole-cell configuration. A pair of images were recorded during the 2^{nd} half of each pulse, during a steady-state. The patch-clamp-imaging setup was described in detail by Wigoda et al. (2017), except for the current substitution with the abovementioned Eclipse microscope and IXON camera. This calibration confirmed the positive correlation between the di-8-ANEPPS fluorescence ratio and depolarization (Suppl. Fig.8).

Solutions. Di-8-ANEPPS (Molecular probes, Life technologies, cat. # D3167, Oregon, USA): a 10 mM stock solution in DMSO was stored in 10 µL aliquots at -20 °C.

Pluronic F-127 (Molecular probes, Life technologies, cat. # P6867, Oregon, USA), a 20% stock solution in DMSO was stored in 100 uL aliquots at RT. °C.

Bath Solution (in mM): 5 KCl, 1 $CaCl_2$, 4 $MgCl_2$, 10 MES; pH 5.6; osmolality: 435 mOsm, adjusted w/ D-sorbitol.

Patch-clamp pipette solution (in mM):112 K-Gluconate, 28 KCl. 2 $MgCl_2$, 10 HEPES, 328 Sorbitol, pH 7.5, Osmolarity: 480 mOsm

Tyrphostin 9 was added to the bath solution from aliquots used in the detached leaves experiments.

Leaf vein density measurements – vein density measurements were performed as in Grunwald et al., 2020.

Osmotic water permeability coefficient (P_f) determination under different light regimes

Protoplast isolation and P_f determination were performed on *SCR:GFP* (Col) as already described (Shatil-Cohen et al., 2014) with the following modifications: The P_f determination by the hypo-osmotic challenge (150 mOsm less than in the isotonic solution) was carried out under either light (6 V-30 W halogen lamp, PHILIPS 5761) or dark treatment.

Light treatments: After isolation, the protoplasts were divided in two tubes, one tube ("light treated") was kept in constant light in the growth room and the other tube ("dark treated") was kept in a light-proof box until the measurements. The light source during the hypo-osmotic challenge of the light-treated protoplasts was the built-in microscope bulb. During the osmotic challenge of the dark-treated protoplasts, the room was darkened, protoplasts were added to the experimental chamber and let sink and stick to the bottom, and a GFP-positive BSC was quickly located. Next, the microscope light was turned off, and the cell was kept in the chamber in total darkness for 10 minutes. During the 1 min videotaping of

the protoplast's hypoosmotic challenge, the chamber was illuminated by the microscope lamp via a red plastic band-pass filter (~600-700nm/ 30 μmol m^{-2} sec^{-1}) to block the BL. Henceforth, in P_f experiments, we designate this low-level red light illumination as "Dark". Both wash solutions (isotonic and hypotonic) were buffered to pH 5.7.

Determination of guttation drops pH

Whole intact WT (Col) plants were covered overnight with black plastic bags to increase the relative humidity in their atmosphere and to prevent transpiration. The following morning immediately after the growth room lights went ON), guttation droplets were collected from the tips of the leaves. Ten to twenty guttation droplets were collected and pooled to reach a sample volume of approximately 20 μL in a 200-μL vial, which was immediately sealed. pH was measured within 10 min of sample collection using a micro-pH electrode MI-410 (Microlectrode, Inc., New Hampshire, USA).

RESULTS

PHOT1 and PHOT2 light receptors are involved in K_{leaf} regulation

Following the GC model in which the photoreceptors PHOT1 and PHOT2 transduce the BL stomatal opening signal, and encouraged by the substantial expression of the blue light receptor genes *PHOT1* and *PHOT2* in the Arabidopsis BSCs transcriptome (Wigoda et al., 2017), we explored the role of these two light receptors in the regulation of the leaf hydraulic conductance, K_{leaf}. We compared, under two light regimes, red light (RL) and red light + blue light (RL+ BL), the K_{leaf} of WT plants to K_{leaf} of knockout mutants lacking one or both of these light receptors (*phot1-5, phot 2-1 and phot1-5 phot 2-1*; Fig. 1). Under RL+BL, WT leaves' K_{leaf} was more than 3-fold higher than under RL treatment and more than 2-fold higher than K_{leaf} of the RL+BL-treated three mutants. Also, under RL+BL, *phot 2-1* mutant's K_{leaf} was about 40 % higher than under the RL treatment. In contrast, BL did not seem to increase the *phot1-5* mutant's or the double mutant's K_{leaf} compared to K_{leaf} under the RL treatment. Under RL, K_{leaf} did not differ among all the mutants, but while the WT's K_{leaf} was no different than the single-mutants' K_{leaf}, it was about double that in the double mutant (Fig. 1).

The higher calculated value of WT's K_{leaf} under BL (as compared to RL), resulted from a greatly increased (less negative) leaf water potential, Ψ_{leaf}, and an appreciably higher transpiration rate, E (Eq. 1, Materials and methods). This invites the interpretation that the BL-induced a highly conductive water pathway into the leaf enabling higher radial water influx which, in turn, was able to compensate for the BL-enhanced E, i.e. water efflux from the leaf, via the BL-increased stomata conductance, g_S (suppl. Fig. S1).

BSCs-specific silencing of PHOT1 and PHOT2 receptors decreased K_{leaf}

To examine specifically the participation of the BSCs' light receptors in the BL-induced K_{leaf} increase, we silenced either the *PHOT1* or the *PHOT2* gene using amiRNA (artificial microRNA) under the BSCs-specific promoter, *SCARECROW* (*SCR*, see Materials and Methods). Under RL+BL illumination, the K_{leaf} values of leaves of both types of transgenic plants, *SCR:mirphot1* and *SCR:mirphot2*, were lower (by 40 -50 %) than the K_{leaf} values of WT leaves (Fig. 2). In contrast, all the *SCR:mirphot* plants had WT'-like g_s and E, while their Ψ_{leaf} was lower (by 50-90 %) than WT's suggesting the reduction of radial water influx to the leaf (Suppl Fig. S2).

BSCs-specific complementation of the *phot1-5* mutant with PHOT1 restored K_{leaf}

We complemented the *phot1-5* (Col-gl) mutant plants with *SCR*:*PHOT1* to restore PHOT1 activity exclusively in the BSCs (Materials and Methods) and compared them to WT (Col-gl) plants and to *phot1-5* plants. *SCR*:*PHOT1* plants illuminated with RL+BL had their K_{leaf} restored from *phot1-5* values to WT values (Fig. 3). While, as expected, BL increased the WT's g_S , the mutant's g_S and that of the complemented mutant did not change under BL also as expected from the main-BL-receptor-devoid guard cells (Suppl. Fig. S3). Notably, under BL, the Ψ_{leaf} of the *SCR*:*PHOT1* complemented mutant was restored to the WT's values, and both were higher by over 50% than the mutant's Ψ_{leaf} (Suppl. Fig. S3). This was the major contribution to the restored high K_{leaf} of the complemented mutant, suggesting a restoration of radial water influx to the leaf.

The kinase inhibitor, tyrphostin 9, inhibited the RL+BL-induced K_{leaf} increase

The kinase inhibitor tyrphostin 9 suppressed the blue-light-dependent H^+-ATPase phosphorylation in guard cells (Hayashi et al., 2017). To examine further whether the vascular PHOT receptors initiate a similarly sensitive phosphorylating event in the BL-

dependent K_{leaf} regulation pathway, we perfused detached WT leaves with AXS, without or with 10 μM tyrphostin 9, and exposed them to RL or RL+BL treatments (Materials and Methods). The K_{leaf} values of RL+BL-illuminated leaves perfused with tyrphostin 9 were about 50% lower than in RL+BL-illuminated control leaves (without tyrphostin 9), and were no different than K_{leaf} in leaves illuminated with RL only (whether or not exposed to tyrphostin 9; Fig.4a, left panel, suppl. Fig S5). However, g_S was not affected by the petiole-fed tyrphostin 9 (Fig.4b, left panel). In contrast to the perfused tyrphostin 9, spraying the inhibitor on the leaf surface did not interfere with the BL-induced almost 3-fold K_{leaf} increase (Fig. 4a, right panel) but it averted the BL-induced g_S increase (Fig. 4b, right panel). The impaired stomatal response as a result of tyrphostin 9 application directly on the leaf surface, is in agreement with (Hayashi et al., 2017) findings in which tyrphostin 9 inhibited BL stomatal opening in epidermal peels. The leaf transpiration, E, behaved in a pattern similar to g_S (Suppl. Fig S4a). Petiole-fed tyrphostin 9 abolished the BL-induced increase of Ψ_{leaf}, but tyrphostin 9 sprayed on the leaf surface did not prevent it (Suppl. Fig S4b).

BL hyperpolarizes the BSCs

To investigate further whether the BSCs plasma-membrane H^+-ATPases plays a role in the BL signal transduction pathway, resembling GCs, we monitored the membrane potential of BSC protoplasts using the potentiometric dual-excitation dye di-8-ANEPPS. Indeed, 5-10 min of RL+BL illumination hyperpolarized the BSCs protoplasts relative to RL illumination or to Dark (absence of illumination), while 10 μM tyrphostin 9 added in the bath (Materials and Methods) not only abolished the BL-induced hyperpolarization but even depolarized the BSCs (Fig. 5, Suppl. Fig. S8), linking BL to the activity of plasma membrane proton pumps.

AHA2 plays a role in the BL-induced K_{leaf} regulation

Recently, we reported that AHA2 plays a major role in K_{leaf} regulation by acidifying the xylem sap. To test further whether the BSC's H^+-ATPase AHA2 participates in the blue light-initiated K_{leaf} regulation pathway, we examined the AHA2 knockout mutant *aha2-4*, and its BSCs-complemented transgenic plant line *SCR*:*AHA2* (i.e., the *aha2-4* mutant with AHA2 expressed only in its BSCs (Grunwald et al., 2020)) under the two light regimes (RL and RL+BL). K_{leaf} of *aha2-4* leaves did not respond to the RL+BL illumination and was only about 40 % of K_{leaf} of the BL-treated WT leaves, but, a similar illumination increased K_{leaf} of the AHA2-complemented (*SCR*:*AHA2*) plants to almost 65 % of the WT's K_{leaf} (Fig. 6), indicating that the BL-induced K_{leaf} increase depended on AHA2. In contrast, under RL+BL, E and g_S of *SCR*:*AHA2* did not differ from E and g_S of the *aha2-4* mutant, and they remained unaffected by BL and lower than the WT's E and g_S (Suppl. Fig S5a & b). Notably, Ψ_{leaf} of *SCR*:*AHA2* was higher by about 40 % than the mutant's and did not differ from the WT's Ψ_{leaf} suggesting a restoration of radial water influx to the leaf (Suppl. Fig S5c).

Morning light after night darkness acidifies the xylem sap

In order to find out whether – like in GCs – the BSC apoplast, i.e., the xylem sap, is more alkaline at night and changes to more acidic in the morning, we first measured the pH of guttation drops collected from the tips of WT leaves before "dawn" (i.e., before lights-ON, Materials and Methods) and found that their mean pH was 7.3. Next, we measured the xylem sap pH in detached leaves, comparing leaves before dawn to leaves after dawn (i.e., leaves at the end of an overnight dark treatment, to leaves after a 30 min WL illumination in the growth chamber; Materials and Methods). This comparison included leaves of WT, *phot1-5* and *SCR:PHOT1* plants. Illumination acidified the xylem sap in WT plants by approx. 0.6 pH units, from 6.0 to 5.4 and in the *SCR: PHOT1* plants by approx. 0.8 pH

364 units, from 6.1 to 5.3, while the xylem pH in *phot1-5* remained unchanged, at about 5.9
365 (Fig. 7), suggesting that PHOT1 in the BSCs is necessary for light-activated xylem
366 acidification.

367 **Light increases the osmotic water permeability, P_f, of the BSCs**

368 To delve further into the link between light and K_{leaf}, we tested whether light affects the
369 osmotic water permeability (P_f) of the BSCs membrane. We determined the P_f of isolated
370 BSC protoplasts from videotapes of their swelling during a hypotonic challenge after white
371 light (WL) illumination or after darkening for 10 min (Materials and Methods). The
372 illuminated BSCs had higher P_f than the dark-treated ones (Fig. 8), suggesting that light is
373 necessary for the increased water fluxes from the xylem to the mesophyll at first light.

374 **Leaf vein architecture is not affected by the expression of PHOT1 or PHOT2**

375 In order to rule out that the diminished K_{leaf} in response to BL of the Phot receptor mutants
376 we observed, were dew to differences in leaf architecture and morphology, we quantified
377 the vein density in all lines we studied and found no differences among them (Suppl. Fig
378 S9).

379

380

381

DISCUSSION

BL signal transduction in the BSCs compared to the GC's BL signal transduction

Stomatal opening, as well as chloroplasts movement in response to BL (Zeiger et al., 1983; Sakai et al., 2001) are considered the outcomes of a "classical" short-term BL-induced signaling pathway mediated by PHOT1 and PHOT2 photoreceptors (Kinoshita et al., 2001b; and reviewed by Briggs and Christie, 2002).

We argue here that a similar and autonomous BL signaling mechanism underlies the increase of K_{leaf} by BL in Arabidopsis. To explain the underlying mechanism, we build on our earlier findings that, on the one hand, the BSCs express substantial levels of *PHOT1* and *PHOT2* receptors (Wigoda et al., 2017) and, on the other hand, K_{leaf} is enhanced by xylem sap acidification by the BSCs' AHA2 (Grunwald et al., 2020). Here, we link these findings using the PHOT receptors mutants *phot1-5* and *phot2-1*, and the double mutant *phot1-5 phot2-1*, and, moreover, we focus on the roles of both receptors PHOT1 and PHOT2 specifically in the BSCs and demonstrate the independence of the BSCs' BL signaling from the GCs' BL signaling. This notion of independence is particularly important since the BSC layer constitutes a hydraulic valve between the xylem and the leaf, regulating water loss to the atmosphere *in series* with the GCs apertures.

The similarity of BSCs BL-signaling to the stomata-opening BL-signaling, is highlighted by the requirement for the presence of both active PHOT1 and PHOT2 receptors for the BL-induced increase of K_{leaf} and g_S; we base this conclusion on the particularly severe depression of both responses in the double mutant relative to the two single mutants' responses (13 % of the WT's K_{leaf} BL response remaining in the double mutant, vs 32 and 40 % of the WT's K_{leaf} in *phot1-5* and in *phot2-1*, respectively (Fig.1), and 35% of the WT's g_S BL response remaining in the double mutant, vs 57 % and 71% of the WT's g_S in *phot1-*

406 *5* and in *phot2-1*, respectively (Suppl. Fig.S1a; similar BL effects on stomatal apparture in
407 these mutants have been reported earlier (Kinoshita et al., 2001)).
408 Similar between the two systems (BSCs and GCs) is also the slightly higher sensitivity to
409 BL in the *phot2-1* mutant seen both in K_{leaf} (Fig.1) and in g_S (Suppl. Fig.S1a), the latter also
410 already noted earlier (Kinoshita et al., 2001), and both likely due to the presence of PHOT1.
411 Notably, based on the complete abolishment of the BL-K_{leaf} response in the *phot1-5* mutant,
412 PHOT2 would appear completely redundant, were it not for the even more severe
413 impairment of the double mutant's K_{leaf} (even below the WT's K_{leaf} under RL alone) (Fig.1).
414 Interestingly, after 2-4 hours of illumination (beyond our usual 15 minutes of illumination)
415 the *phot* single mutants's g_S re-acquired the WT-like BL sensitivity (Suppl. Fig. S7), similar
416 to an earlier report on stomatal aperture after 2-4 hours of BL illumination (Kinoshita et al.,
417 2001); this could perhaps reflect a gradually accumulating effect of the GCs' AHA activity,
418 overcoming the partially impaired PHOT-to-AHA signal transduction in the single *phot*
419 mutants.
420 That the PHOTs (and particularly PHOT1) are indispensible to BL signaling in the BSCs,
421 as they are in GCs, is emphasized additionally by our two genetic manipulations focused
422 entirely on the BSCs: (a) the severe impairment of the BL-induced K_{leaf} increase in WT
423 plants with either PHOT1 or PHOT2 silenced by *SCR:PHOT-mirs* (Fig. 2) and (b) the full
424 restoration of K_{leaf} sensitivity to BL by *phot1-5* complementation with *SCR:PHOT1* (Fig.
425 3).
426 While the results of these genetic manipulations on the BSCs PHOTs attest, importantly,
427 to their involvement in the BL regulation of radial water influx to the leaf, they also

emphasize the independence of the BSCs BL signal transduction from that in the GCs – as deduced from the lack of their effect on the g_S (Suppl. Figs. S2a, S3a).

Additionally, the localized effects of the PHOT inhibitor, tyrphostin 9 demonstrated both the similarity between the BSCs' and the GC's BL signaling pathways in WT plants and the independence of the first from the latter; both signaling pathways were inhibited by it, but only when it was applied in close proximity to the tissue of action: BSCs were affected only by the petiole-fed tyrphostin 9, which inhibited the BL-induced increase of K_{leaf} and Ψ_{leaf} without affecting g_S, while GCs were affected only by tyrphostin 9 sprayed on the leaf surface (i.e., on GCs), which abolished the BL-induced g_S increase without affecting K_{leaf} (Fig.4, suppl. Fig. S4).

The cellular BL signal transduction pathway of the BSCs

The BSCs hyperpolarization in response to BL that we observed (Fig. 5) resembles the GCs hyperpolarization in response to BL (Assmann et al., 1985; Roelfsema et al., 2001; Taylor and Assmann, 2001) and its inhibition by tyrphostine (Fig. 5) suggests the involvement of the PHOT receptors in a similar way (Hayashi et al., 2017). Hyperpolarization is known to be generated by the plasma membrane H^+-ATPase activity (Spanswick, 1981). Recently we reported that the BSCs H^+-ATPase plays a major role in the acidification of the xylem sap which in turn increases K_{leaf} (Grunwald et al., 2020). Indeed – compared to WT – the H^+-ATPase mutant, *aha2-4* had a diminished BL-induced K_{leaf} increase (possibly due to a more alkaline xylem pH), as well as a diminished BL-induced g_S increase, while *aha2-4* with the *SCR:AHA2* complementation limited to BSCs had its BL-induced K_{leaf} increase restored, while its g_S remained unaffected, affirming the mediation by *AHA2* of the BL increase of K_{leaf} (Fig. 6, Suppl. Fig. S6). Notably, this is an interesting contrast with the otherwise similar GCs' BL-signaling pathway, which terminates upon AHA1 (Yamauchi et al., 2016).

Previously, we also reported (Grunwald et al., 2020) that the regulation of K_{leaf} by the xylem sap pH was mediated via the effect of the BSCs apoplastic pH (i.e., of the xylem sap pH) on their osmotic water permeability, P_f. We showed that the BSCs P_f increased when the apoplastic pH declined due to the BSCs H^+-ATPase activity. Here, we report that, in addition to external low pH, light is also needed for the BSCs P_f increase (Fig.8). The role of BSCs aquaporins in controlling K_{leaf} was already identified earlier (in walnut, Ben Baaziz et al., 2012; in grapevine, Vitali et al., 2016; in poplar, Muries et al., 2019; in Arabidopsis, Sade et al., 2014; Prado et al., 2019). In particular, Prado et al., (2019) demonstrated a contribution of the abundant – also in the leaf veins – aquaporin AtPIP2;1 to the rhythmicity of the diurnal and circadian hydraulic conductance of the Arabidopsis rosette, K_{ros}, which peaked before mid-day. Thus, in addition to the likely P_f-promoting effect of the slightly acidic pH (6) perfusion solution (YG,NW et al., 2020) that Prado et al. (2019) used in their K_{ros} measurements, the changes in K_{ros} reflected also the effects of light and the circadian clock (Prado et al., (2019).

Elaborating on the correlation between K_{ros} and AtPIP2;1 phosphorylation that they found, these authors demonstrated that frog oocytes expressing AtPIP2;1 had higher P_f induced by co-expressing two of the Arabidopsis 14-3-3 protein isoforms which bound to the AtPIP2;1 (Prado et al., 2019). It would be tempting to speculate, on this basis, that, resembling the PHOT-initiated BL signaling cascade involving 14-3-3 proteins which bind to and upregulate the GCs' AHA1 activity (e.g., Emi et al., 2001) also AtPIP2;1 activity, and perhaps that of other vascular aquaporins may be enhanced by light via similar signaling (i.e., by phosphorylation and 14-3-3 protein binding).

An alternative tempting speculation would be that the light-induced BSCs' P_f increase is due to BL-mediated activation ofAHA2 and the BSCs' cytosol alkalinization resulting from

476 proton secretion. Earlier work already documented that P_f increases due to aquaporin
477 activation by cytosol alkalinization, mediated by conserved histidine (His 197 in AtPIP2;2;
478 Tournaire-Roux et al., 2003) and a leucine (Leu206 in BvPIP2;2 Fortuna et al., 2019) in
479 the cytosol-facing D loop of the aquaporin protein. Moreover, could the concurrent
480 hyperpolarization of BSCs by BL (also via AHA2 activation) imply a possible role of
481 hyperpolarization in the regulation of the BSCs AQPs as suggested by in-silico simulations
482 (Hub et al., 2010)? This possibility needs yet to be explored experimentally.

483 The model of K_{leaf} activation by BL, in a GC-like BL signal transduction pathway, that our
484 results support, is as follows: the BSCs' PHOT1 and PHOT2 (only partially redundant)
485 perceive the blue light, activate the plasma membrane H^+-ATPase (AHA2), which
486 hyperpolarizes the BSCs and acidifies the xylem pH, leading to an increase of the BSC P_f
487 and, in turn, to a rise of K_{leaf}, or, schematically:

488 **BL →BSCs' *PHOT*s activation →tyrosin phosphorylation* →BSCs' H^+-ATPase**
489 **(AHA2) activation →BSCs hyperpolarization and xylem acidification → BSCs P_f**
490 **elevation →K_{leaf} increase.**

491 * Notably, the abovementioned tyrosine phosphorylation step – suggested to occur, in the
492 guard cells, on the BHP protein upstream of the H^+-ATPase (Hayashi et al., 2017) – is yet
493 to be explored in the BSCs; currently, our guess is that similarly to the GC, this step occurs
494 upstream of the BSCs' AHA2 (Fig. 9).

495 **The physiological relevance of K_{leaf} increase by blue light**

496 Both GCs opening and K_{leaf} increase occur in the early morning hours (e.g., Brodribb and
497 Holbrook, 2004; Domec et al., 2009; Locke and Ort, 2015) when the irradiance spectrum
498 is relatively enriched in blue wavelengths (Chiang et al., 2019, Matthews et al., 2020, and
499 references therein). We suggest that the advantage of this blue light response of stomata is

in allowing the acquisition of CO_2 during sub-maximum VPD (vapor pressure deficit, a measure of the driving force for leaf water evaporation), thus increasing water use efficiency (WUE).

What is the advantage of such early K_{leaf} response to light?

Interestingly, not only does K_{leaf} increase in response to blue light as does stomatal aperture but, in accord with our conclusions about the independence of the BSCs' BL signal transduction from that of the GCs', K_{leaf} responds to light faster than g_S (Guyot et al., 2012). One possible advantage of this, could be to match stomata opening with increased water flux into the leaf. Were it not for this accompanying K_{leaf} increase, BL-induced stomata opening, which peaks in the morning hours (the "Golden hour"; Gosa et al., 2018), could accumulate an imbalance of leaf water, even in the presence of a relatively low VPD, leading to a drop in the leaf water potential (Ψ_{leaf}); this in turn, could close stomata (Raschke, 1970; Guyot et al., 2012; Klein, 2014; Scoffoni et al., 2018) and thus limit photosynthesis. Instead, an early morning increase of K_{leaf} would elevate Ψ_{leaf} thereby increasing and prolonging the opening stomata (ibid). Thus, the BL-response of K_{leaf} could support and enhance the stomata BL response. Hypothetically, under more extreme conditions, e.g., with high VPD already in the early morning, increased K_{leaf} would prevent a hydraulic pathway failure when stomatal conductance is at its peak (Brodribb and Holbrook, 2004; Halperin et al., 2017; Gosa et al., 2019).

Another possible advantage of the early morning BL-induced K_{leaf} increase may be related to CO_2 permeability via aquaporins. A few lines of evidence converge to support this hypothesis: (a) CO_2 can cross cell membranes through aquaporins, and, in particular, those of the PIP1 family, and (b) the transcripts of PIP1 family aquaporins were upregulated concomitantly with K_{leaf} increase in walnut by white light illumination (as short as a 15 min; Biaaziz et al., 2012), (c) in soybean, the transcript of a PIP1 family aquaporin (PIP1;8)

was more abundant in the morning than in midday in correlation with a higher K_{leaf} in the morning than in the midday (Locke and Ort, 2015), (d) we demonstrated that aquaporins control K_{leaf} (Shatil-Cohen and Moshelion, 2012; Sade et al., 2014); (e) xylem-transported CO_2 could be a source for CO_2 assimilated in the bundle sheath and mesophyll (Janacek et al., 2009; Hubeau et al., 2019). Thus, assuming the K_{leaf} increase with the first light of day parallels the increase of CO_2 permeability of aquaporins in the BSCs, the passage to the mesophyll of CO_2 from the xylem originating in roots respiration will be enhanced even before full stomatal opening. The increased CO_2 availability at this time, when the photosynthetic light is already sufficient, would enhance CO_2 assimilation – a great advantage to the plant. Interestingly, photosynthetic CO_2 uptake reaches a maximum within 10 minutes of blue light (Doi et al., 2015), which is over threefold faster than the full opening of stomata (Grondin et al., 2015). In conclusion, our data provide new evidence for the role of the BSCs' phototropins (PHOT1 and PHOT2) in their AHA2-mediated increase of K_{leaf} by blue light.

An additional interesting outcome from our results is the corroboration – and explanation – of the reports on alkalinized xylem sap pH in the absence of light, e.g., at night (Urrestarazu et al., 1996 (in tomatoes); Aubrey et al., 2011 (in poplars)), or even on cloudy days (in poplars; Aubrey et al., 2011). Similarly, in Arabidopsis, only after dawn and the activation of the BL signal transduction pathway does the xylem sap become acidic (as in Fig.7) and K_{leaf} increases (Fig. 3).

Our results, together with the fact that in the dark the BSC P_f is low (Fig. 8), may explain how the mesophyll does not get flooded at night when root pressure increases. While during day time the BSCs' higher P_f underlies the higher K_{leaf} which is important for the support of transpiration (Sade et al., 2015; Shatil-Cohen and Moshelion, 2012; Grunwald et al., 2020; Sade et al., 2014), at night, the P_f and K_{leaf} reduction likely prevents water influx into

the leaf, and the buildup of root pressure is relieved via guttation, and if not — xylem sap may flood the leaf (Shatil-Cohen and Moshelion, 2012). Not surprisingly, and in accord with the dark-alkalinization of the xylem sap, guttation drops pH was 7.2 ± 0.04 (±SE, 15 biological repeats/ collected over three days).

The inactivity of the BSCs H^+-ATPases, manifested in the nightly alkalinization of the xylem sap, could be advantageous for the plant as a means of energy conservation, as ATPases operate at a high energetic cost (Palmgren, 2001).

These findings expand our understanding of the molecular basis of the leaf water influx regulation. That BL increases K_{leaf} in several other species (Voicu et al., 2008; Voicu et al., 2009; Sellin et al., 2011; Aasamaa and Sber, 2012; Ben Baaziz et al., 2012), imparts an even more general importance to our results. Thus, a focus on the hydraulic valve in series with the stomata should provide new directions for studying the plant water relations within its environment.

REFERENCES

Aasamaa, K. and Sõber, A. (2012). Light sensitivity of shoot hydraulic conductance in five temperate deciduous tree species. Funct. Plant Biol. **39**: 661.

Abràmoff, M.D., Magalhães, P.J., and Ram, S.J. (2004). Image processing with imageJ. Biophotonics Int. **11**: 36–41.

Alvarez, J.P., Pekker, I., Goldshmidt, A., Blum, E., Amsellem, Z., and Eshed, Y. (2006). Endogenous and Synthetic MicroRNAs Stimulate Simultaneous, Efficient, and Localized Regulation of Multiple Targets in Diverse Species. Plant Cell **18**: 1134–1151.

Assmann, S. (1993). Signal Transduction in Guard Cells. Annu. Rev. Cell Dev. Biol. **9**: 345–375.

575 **Assmann, S.M., Simoncini, L., and Schroeder, J.I.** (1985). Blue light activates
576 electrogenic ion pumping in guard cell protoplasts of Vicia faba. Nature **318**: 285–287.
577 **Aubrey, D.P., Boyles, J.G., Krysinsky, L.S., and Teskey, R.O.** (2011). Spatial and
578 temporal patterns of xylem sap pH derived from stems and twigs of Populus deltoides L.
579 Environ. Exp. Bot. **71**: 376–381.
580 **Ben Baaziz, K., Lopez, D., Rabot, A., Combes, D., Gousset, A., Bouzid, S., Cochard,**
581 **H., Sakr, S., and Venisse, J.-S.** (2012). Light-mediated Kleaf induction and contribution
582 of both the PIP1s and PIP2s aquaporins in five tree species: walnut (Juglans regia) case
583 study. Tree Physiol. **32**: 423–434.
584 **Briggs, W.R. and Christie, J.M.** (2002). Phototropins 1 and 2: Versatile plant blue-light
585 receptors. Trends Plant Sci. **7**: 204–210.
586 **Briggs, W.R. and Huala, E.** (1999). Blue-Light Photoreceptors in Higher Plants. Annu.
587 Rev. Cell Dev. Biol. **15**: 33–62.
588 **Brodribb, T.J. and Holbrook, N.M.** (2004). Diurnal depression of leaf hydraulic
589 conductance in a tropical tree species. Plant, Cell Environ. **27**: 820–827.
590 **Chiang, C., Olsen, J.E., Basler, D., Bånkestad, D., and Hoch, G.** (2019). Latitude and
591 Weather Influences on Sun Light Quality and the Relationship to Tree Growth. Forests
592 **10**: 610.
593 **Clough, S.J. and Bent, A.F.** (1998). Floral dip: A simplified method for Agrobacterium-
594 mediated transformation of Arabidopsis thaliana. Plant J. **16**: 735–743.
595 **Doi, M., Kitagawa, Y., and Shimazaki, K.-I.** (2015). Stomatal Blue Light Response Is
596 Present in Early Vascular Plants. Plant Physiol. **169**: 1205–1213.
597 **Domec, J.C., Noormets, A., King, J.S., Sun, G., McNulty, S.G., Gavazzi, M.J., Boggs,**
598 **J.L., and Treasure, E.A.** (2009). Decoupling the influence of leaf and root hydraulic
599 conductances on stomatal conductance and its sensitivity to vapour pressure deficit as soil

dries in a drained loblolly pine plantation. Plant, Cell Environ. **32**: 980–991.

Elmore, J.M. and Coaker, G. (2011). The Role of the Plasma Membrane H+-ATPase in Plant–Microbe Interactions. Mol. Plant **4**: 416–427.

Emi, T., Kinoshita, T., and Shimazaki, K. (2001). Specific binding of vf14-3-3a isoform to the plasma membrane H+-ATPase in response to blue light and fusicoccin in guard cells of broad bean. Plant Physiol. **125**: 1115–1125.

Fortuna, C.A., Zerbetto De Palma, G., Aliperti Car, L., Armentia, L., Vitali, V., Zeida, A., Estrin, D.A., and Alleva, K. (2019). Gating in plant plasma membrane aquaporins: the involvement of leucine in the formation of a pore constriction in the closed state. FEBS J. **286**: 3473–3487.

Gosa, S.C., Lupo, Y., and Moshelion, M. (2019). Quantitative and comparative analysis of whole-plant performance for functional physiological traits phenotyping: New tools to support pre-breeding and plant stress physiology studies. Plant Sci. **282**: 49–59.

Grondin, A., Rodrigues, O., Verdoucq, L., Merlot, S., Leonhardt, N., and Maurel, C. (2015). Aquaporins Contribute to ABA-Triggered Stomatal Closure through OST1-Mediated Phosphorylation. Plant Cell **27**: 1945–1954.

Grunwald, Y., Wigoda, N., Sade, N., Yaaran, A., Torne, T., Gosa, S.C., Moran, N., and Moshelion, M. (2020). Arabidopsis leaf hydraulic conductance is regulated by xylem-sap pH, controlled, in turn, by a P-type H+-ATPase of vascular bundle sheath cells. bioRxiv: 234286.

Guyot, G., Scoffoni, C., and Sack, L. (2012). Combined impacts of irradiance and dehydration on leaf hydraulic conductance: insights into vulnerability and stomatal control. Plant. Cell Environ. **35**: 857–871.

Halperin, O., Gebremedhin, A., Wallach, R., and Moshelion, M. (2017). High-throughput physiological phenotyping and screening system for the characterization of

plant-environment interactions. Plant J. **89**: 839–850.

Hayashi, M., Inoue, S., Ueno, Y., and Kinoshita, T. (2017). A Raf-like protein kinase BHP mediates blue light-dependent stomatal opening. Sci. Rep. **7**: 45586.

Hsiao, T.C., Allaway, W.G., and Evans, L.T. (1973). Action Spectra for Guard Cell Rb + Uptake and Stomatal Opening in Vivia faba. Plant Physiol. **51**: 82–88.

Hub, J.S., Aponte-Santamaría, C., Grubmüller, H., and De Groot, B.L. (2010). Voltage-regulated water flux through aquaporin channels in silico. Biophys. J. **99**: L97–L99.

Hubeau, M., Thorpe, M.R., Mincke, J., Bloemen, J., Bauweraerts, I., Minchin, P.E.H., De Schepper, V., De Vos, F., Vanhove, C., Vandenberghe, S., and Steppe, K. (2019). High-Resolution in vivo Imaging of Xylem-Transported CO2 in Leaves Based on Real-Time 11C-Tracing. Front. For. Glob. Chang. **2**: 25.

Van Ieperen, W., Savvides, A., and Fanourakis, D. (2012). Red and blue light effects during growth on hydraulic and stomatal conductance in leaves of young cucumber plants. Acta Hortic. **956**: 223–230.

Janacek, S.H., Trenkamp, S., Palmer, B., Brown, N.J., Parsley, K., Stanley, S., Astley, H.M., Rolfe, S.A., Paul Quick, W., Fernie, A.R., and Hibberd, J.M. (2009). Photosynthesis in cells around veins of the C 3 plant Arabidopsis thaliana is important for both the shikimate pathway and leaf senescence as well as contributing to plant fitness. Plant J. **59**: 329–343.

Karlsson, P.E. (1986). Blue light regulation of stomata in wheat seedlings. II. Action spectrum and search for action dichroism. Physiol. Plant. **66**: 207–210.

Kinoshita, T., Doi, M., Suetsugu, N., Kagawa, T., Wada, M., and Shimazaki, K. (2001). Phot1 and Phot2 mediate blue light regulation of stomatal opening. Nature **414**: 656–660.

Kinoshita, T. and Shimazaki, K. (1999). Blue light activates the plasma membrane H+-ATPase by phosphorylation of the C-terminus in stomatal guard cells. EMBO J. **18**: 5548–5558.

Klein, T. (2014). The variability of stomatal sensitivity to leaf water potential across tree species indicates a continuum between isohydric and anisohydric behaviours. Funct. Ecol. **28**: 1313–1320.

Kronenberg, G.H.M. and Kendrick, R.E. (1986). The physiology of action. In Photomorphogenesis in plants (Springer Netherlands: Dordrecht), pp. 99–114.

Locke, A.M. and Ort, D.R. (2015). Diurnal depression in leaf hydraulic conductance at ambient and elevated [CO2] reveals anisohydric water management in field-grown soybean and possible involvement of aquaporins. Environ. Exp. Bot. **116**: 39–46.

Matthews, J.S., Vialet-Chabrand, S., Lawson, T., and Evans, J. (2020). Role of blue and red light in stomatal dynamic behaviour. J. Exp. Bot. **71**: 2253–2269.

Muries, B. et al. (2019). Aquaporins and water control in drought-stressed poplar leaves: A glimpse into the extraxylem vascular territories. Environ. Exp. Bot. **162**: 25–37.

Negin, B. and Moshelion, M. (2017). The advantages of functional phenotyping in pre-field screening for drought-tolerant crops. Funct. Plant Biol. **44**: 107.

Oishi, A.C., Oren, R., Novick, K.A., Palmroth, S., and Katul, G.G. (2010). Interannual Invariability of Forest Evapotranspiration and Its Consequence to Water Flow Downstream. Ecosystems **13**: 421–436.

Den Os, D., Staal, M., and Elzenga, J.T.M. (2007). Signal integration by ABA in the blue light-induced acidification of leaf pavement cells in pea (Pisum sativum L. var. Argenteum). Plant Signal. Behav. **2**: 146–152.

Palmgren, M.G. (2001). Plant plasma membrane H+ATPases: Powerhouses for nutrient uptake.

675 **Prado, K. and Maurel, C.** (2013). Regulation of leaf hydraulics: from molecular to
676 whole plant levels. Front. Plant Sci. **4**: 1–14.
677 **Raschke, K.** (1970). Stomatal Responses to Pressure Changes and Interruptions in the
678 Water Supply of Detached Leaves of Zea mays L. Plant Physiol. **45**: 415–423.
679 **Roelfsema, M.R.G. and Hedrich, R.** (2005). In the light of stomatal opening: new
680 insights into 'the Watergate.' New Phytol. **167**: 665–691.
681 **Roelfsema, M.R.G., Steinmeyer, R., Staal, M., and Hedrich, R.** (2001). Single guard
682 cell recordings in intact plants: Light-induced hyperpolarization of the plasma membrane.
683 Plant J. **26**: 1–13.
684 **Sade, N., Shatil-Cohen, A., Attia, Z., Maurel, C., Boursiac, Y., Kelly, G., Granot, D.,**
685 **Yaaran, A., Lerner, S., and Moshelion, M.** (2014). The Role of Plasma Membrane
686 Aquaporins in Regulating the Bundle Sheath-Mesophyll Continuum and Leaf Hydraulics.
687 PLANT Physiol. **166**: 1609–1620.
688 **Sade, N., Shatil-Cohen, A., and Moshelion, M.** (2015). Bundle-sheath aquaporins play a
689 role in controlling Arabidopsis leaf hydraulic conductivity. Plant Signal. Behav. **10**:
690 e1017177.
691 **Sakai, A.K. et al.** (2001). The Population Biology of Invasive Species. Annu. Rev. Ecol.
692 Syst.
693 **Schindelin, J. et al.** (2012). Fiji: an open-source platform for biological-image analysis.
694 Nat. Methods **9**: 676–682.
695 **Scoffoni, C., Albuquerque, C., Cochard, H., Buckley, T.N., Fletcher, L.R.,**
696 **Caringella, M.A., Bartlett, M., Brodersen, C.R., Jansen, S., and Mcelrone, A.J.**
697 (2018). The Causes of Leaf Hydraulic Vulnerability and Its Influence on Gas Exchange in
698 Arabidopsis thaliana. **178**: 1584–1601.
699 **Sellin, A., Sack, L., Õunapuu, E., and Karusion, A.** (2011). Impact of light quality on

leaf and shoot hydraulic properties: A case study in silver birch (Betula pendula). Plant, Cell Environ. **34**: 1079–1087.

Shapira, O., Khadka, S., Israeli, Y., Shani, U., and Schwartz, A. (2009). Functional anatomy controls ion distribution in banana leaves: Significance of Na + seclusion at the leaf margins. Plant, Cell Environ. **32**: 476–485.

Shatil-Cohen, A. and Moshelion, M. (2012). Smart pipes. Plant Signal. Behav. **7**: 1088–1091.

Shatil-Cohen, A., Sibony, H., Draye, X., Chaumont, F., Moran, N., and Moshelion, M. (2014). Measuring the osmotic water permeability coefficient (Pf) of spherical cells: isolated plant protoplasts as an example. J. Vis. Exp.: e51652.

Shimazaki, K., Doi, M., Assmann, S.M., and Kinoshita, T. (2007). Light Regulation of Stomatal Movement. Annu. Rev. Plant Biol. **58**: 219–247.

Spanswick, R. (1981). Eelectrogenic ion pumps. Annu. Rev. Plant Physiol. **32**: 67–89.

Svennelid, F., Olsson, A., Piotrowski, M., Rosenquist, M., Ottman, C., Larsson, C., Oecking, C., and Sommarin, M. (1999). Phosphorylation of Thr-948 at the C Terminus of the Plasma Membrane H-ATPase Creates a Binding Site for the Regulatory 14-3-3 Protein.

Takemiya, A., Sugiyama, N., Fujimoto, H., Tsutsumi, T., Yamauchi, S., Hiyama, A., Tada, Y., Christie, J.M., and Shimazaki, K.I. (2013). Phosphorylation of BLUS1 kinase by phototropins is a primary step in stomatal opening. Nat. Commun. **4**.

Talbott, L.D., Shmayevich, I.J., Chung, Y., Hammad, J.W., and Zeiger, E. (2003). Blue Light and Phytochrome-Mediated Stomatal Opening in the npq1 and phot1 phot2 Mutants of Arabidopsis. Plant Physiol. **133**: 1522–1529.

Taylor, A.R. and Assmann, S.M. (2001). Apparent absence of a redox requirement for blue light activation of pump current in broad bean guard cells. Plant Physiol. **125**: 329–

338.

Ueno, K., Kinoshita, T., Inoue, S., Emi, T., and Shimazaki, K. (2005). Biochemical Characterization of Plasma Membrane H+-ATPase Activation in Guard Cell Protoplasts of Arabidopsis thaliana in Response to Blue Light. Plant Cell Physiol. **46**: 955–963.

Urrestarazu, M., Sanchez, A., Lorente, F.A., and Guzmán, M. (1996). A daily rhythmic model for pH and volume from xylem sap of tomato plants. Commun. Soil Sci. Plant Anal. **27**: 1859–1874.

Vitali, M., Cochard, H., Gambino, G., Ponomarenko, A., Perrone, I., and Lovisolo, C. (2016). VvPIP2;4N aquaporin involvement in controlling leaf hydraulic capacitance and resistance in grapevine. Physiol. Plant. **158**: 284–296.

Voicu, M.C., Cooke, J.E.K., and Zwiazek, J.J. (2009). Aquaporin gene expression and apoplastic water flow in bur oak (Quercus macrocarpa) leaves in relation to the light response of leaf hydraulic conductance. J. Exp. Bot. **60**: 4063–4075.

Voicu, M.C., Zwiazek, J.J., and Tyree, M.T. (2008). Light response of hydraulic conductance in bur oak (Quercus macrocarpa) leaves. Tree Physiol. **28**: 1007–1015.

Wigoda, N., Moshelion, M., and Moran, N. (2014). Is the leaf bundle sheath a "smart flux valve" for K+ nutrition? J. Plant Physiol. **171**: 715–722.

Wigoda, N., Pasmanik-Chor, M., Yang, T., Yu, L., Moshelion, M., and Moran, N. (2017). Differential gene expression and transport functionality in the bundle sheath versus mesophyll – a potential role in leaf mineral homeostasis. J. Exp. Bot. **68**: 3179–3190.

Yamauchi, S., Takemiya, A., Sakamoto, T., Kurata, T., Tsutsumi, T., Kinoshita, T., and Shimazaki, K. (2016). Plasma membrane H+-ATPase1 (AHA1) plays a major role in Arabidopsis thaliana for stomatal opening in response to blue light. Plant Physiol.: pp.01581.2016.

Zeiger, E., Assmann, S.M., and Meioner, H. (1983). The Photobiology of Paphiopedilum stomata: opening under blue lightbut not red light. Photochem. Photobiol. **38**: 627–630.

Zeiger, E. and Helper, P.K. (1977). Light and Stomatal Function: Blue Light Stimulates Swelling of Guard Cell Protoplasts. Science (80-.). **196**: 887–889.

FIGURE LEGENDS

Figure 1: The effect of blue light on K_{leaf} of PHOT receptors mutants. K_{leaf} of fully expanded excised leaves of WT (Col-gl) and *PHOT* mutants (*phot1-5* (Col-gl), *phot2-1* (Col-gl) and a double mutant, *phot1-5 phot2-1* (Col-gl)) after illumination for 15 min immediately after dark, with RL (220 µmol m^{-2} s^{-1}), or R+BL (220 µmol m^{-2} s^{-1}, consisting of 90 % RL and 10 % BL; Materials and methods). The columns are mean values (±SE) of the indicated number of biological repeats from three independent experiments. Different letters denote significantly different values (ANOVA, *Post hoc* Tukey's test, $P< 0.05$) . Note the reduced response to RL+BL in the mutant lines.

Figure 2. The effect of RL+BL on the K_{leaf} of PHOT1- and PHOT2-silenced (SCR:mir) plants, generated in WT (Col; Materials and methods). K_{leaf} was determined in fully expanded leaves of WT and *SCR:mirphot1* and *SCR:mirphot2* plants treated with RL or RL+BL (as in Fig. 1; Materials and Methods) The columns are means (± SE) of the indicated number of biological repeats from three independent experiments. Different letters denote significantly different values (ANOVA, Post hoc Tukey's test, $P< 0.05$).

Figure 3. BSCs-directed *PHOT1* complementation of the *phot1-5* mutant restores the normal K_{leaf}. Fully expanded leaves of WT (Col-gl), *phot1-5* and *phot1-5* (Col-gl) plants complemented with *SCR:PHOT1* underwent illumination treatments as in Fig. 1. The columns are means (± SE) of the indicated number of biological repeats from three independent experiments. Different letters denote significantly different values (ANOVA,, *Post hoc* Tukey's test, $P< 0.05$).

Figure 4. Xylem-fed kinase Inhibitor tyrphostin 9 abolished the blue-light-induced K_{leaf} increase and stomatal opening. Fully expanded leaves of WT (Col-gl) were pre-incubated (petiole deep) in AXS without or with tyrphostin 9 (10 µm) or sprayed with AXS without or with tyrphostin 9 (10 µm), and kept overnight in dark boxes. Immediately after dark, leaves were illuminated for 15 min with RL (215 µmolm^{-2} s^{-1} red) or RL+BL (215 µmol m^{-2} s^{-1}, consisting of 90 % RL and 10 % BL). **a.** K_{leaf}. **b.** Stomatal conductance (g_S). The columns are means (± SE) of the indicated number of biological repetitions, determined in three independent experimental days. Different letters denote significantly different values (ANOVA, Post hoc Tukey's test, $P< 0.05$). Note that g_S was reduced when tyrphostin 9 was sprayed but not when fed via the petiole.

Figure 5. - Blue light (BL) hyperpolarizes the BSCs relative to red light (RL) or Dark and tyrphostin 9 depolarizes them. Membrane potential (E_M) of BSC protoplasts, without or with petiole-fed tyrphostin 9 (10 µM), determined using the dual-excitation, ratiometric fluorescent dye di-8-ANEPPS (Materials and Methods). After at least10-20 min in the dark, the cells were immediately imaged (Dark), or illuminated for an additional 5-10 minutes either with RL (220 µmol m^{-2} s^{-1}) or with RL+BL (220 µmol m^{-2} s^{-1}, including 10% BL; Materials and Methods), and then imaged. The columns are mean values of fluorescence ratio (F_{438}/F_{531}) values (±SE; n as indicated) derived from analyses of the images captured at the indicated excitation wavelengths (Materials and Methods) in three independent experiments. Numbers above the columns are the mean values of BSCs E_M, based on a calibration curve of F_{438}/F_{531} vs. E_M obtained in separate experiments using patch clamp (Materials and Methods, Suppl. Fig. S8). Different letters denote significantly different values (ANOVA, Post hoc Tukey's test, $P< 0.05$).

Figure 6. The BSCs H^+-ATPase, AHA2, mediates the blue-light-induced K_{leaf} increase. Fully expanded excised leaves of WT (Col0) plants, *aha2-4* mutant plants (Col0) and *aha2-4* plants complemented in their BSCs with *SCR:AHA2* were illuminated for 15 min immediately after dark, as in Fig.2. The columns are means (± SE) of the indicated number of biological repeats from three independent experiments. Different letters denote significantly different values (ANOVA, Post hoc Tukey's test, $P< 0.05$). Note the marked restoration of K_{leaf} in the *aha2* mutant plants complemented solely in their BSCs.

Figure 7. White light (WL) illumination for 30 minutes acidifies the xylem pH of WT plants and *SCR*:*PHOT1*-complemented mutants, but not in the *phot1-5* mutant. The leaves of WT (Col-gl) plants, *phot1-5* (Col-gl) mutants and the *SCR:PHOT1*-complemented *phot1-5* mutant (as in Fig. 3) were illuminated by the growth room WL (150-200 μmol m^{-2} sec^{-1}, Materials and Methods). The columns are means (±SE) of the indicated number of biological repeats from three independent experiments Different letters denote significantly different values (*Post hoc* Tukey's test, $P< 0.05$).

Figure 8: White light increases the BSCs membrane osmotic water permeability coefficient (P_f). a. A time course of swelling of bundle sheath protoplasts from *SCR:GFP* plants upon exposure to a hypotonic XPS^{db} solution under the same illumination conditions (white light or darkness) as during the light treatment preceding the assay. The bath solution was buffered to pH 5.7. The arrow indicates onset of bath flush. **b.** Time course of the osmotic concentration change in the bath (C_{out}) during the hypotonic challenge **c.** Mean (±SE) initial P_f values of the indicated number of bundle sheath protoplasts under two light regimes from three independent experiments. Columns are means (± SE) of 21-28 biological repetitions, determined in five independent experiments. The asterisk indicates a significant difference (Student's two-tailed unpaired t-test, $P < 0.05$).

Figure 9. Proposed BSCs-autonomous BL signal transduction pathway. a. An artist's rendering of a leaf radial water path, from xylem to mesophyll (K_{leaf}, blue hollow arrow) via the bundle sheath cells, BSCs, which tightly envelop the xylem. GC, a stomata guard cell; MC, mesophyll cell. **b**. Blue-light (BL) signalling pathway (blue arrowheads) in a bundle sheath cell, from BL perception by the phototropin receptors (PHOT), through an intermediate tyrphostin-sensitive tyrosine phosphorylation (TP), to the ultimate AHA2 (orange circle) activation resulting in proton extrusion via the pump and xylem sap

837 acidification, presumably, at the expense of ATP breakdown to ADP with a transient
838 phosphorylation (P) on the pump protein, as expected from a P-type H^+-ATPase.

839

840 **SUPPLEMENTAL FIGURES AND TABLE**

841 **Figure S1**: **PHOT receptors mutants do not show the effect of blue light on the g_S, E**
842 **and Ψ_{leaf}.**

843 **Figure S2. *SCR:mir*-silencing of the PHOT receptors abolishes the effect of RL+BL on**
844 **the g_S, E and Ψ_{leaf}.**

845 **Figure S3. BSCs-directed *PHOT1* complementation of the *phot1-5* mutant elevates**
846 **Ψ_{leaf} but not g_S or E.**

847 **Figure S4**. **Xylem-fed kinase inhibitor tyrphostin 9 does not affect BL-increased E but**
848 **decreases BL-increased Ψ_{leaf}, while tyrphostin 9 sprayed on leaves acts oppositely.**

849 **Figure S5**. **Tyrphostin 9 perfused via the petiole does not affect the physiological**
850 **parameters under RL-only illumination.**

851 **Figure S6. BSCs-directed *AHA2* complementation of the *aha2-4* mutant restores its**
852 **BL-induced Ψ_{leaf} increase but not the BL increases of g_S or E.**

853 **Figure S7. The 'long-illumination' g_S of intact leaves of whole plants does not differ**
854 **among the different genotypes (WT, *phot* mutants and *SCR:PHOT1*).**

855 **Figure S8. *In-situ* calibration of di-8-ANEPPs fluorescence ratio (F-ratio, F_{438}/F_{531})**
856 **vs. the BSCs membrane potential (E_M).**

857 **Figure S9**. **Leaf vein density does not depend on the expression of PHOT1 or PHOT2.**

858 **Table S1: List of primers used in this study**

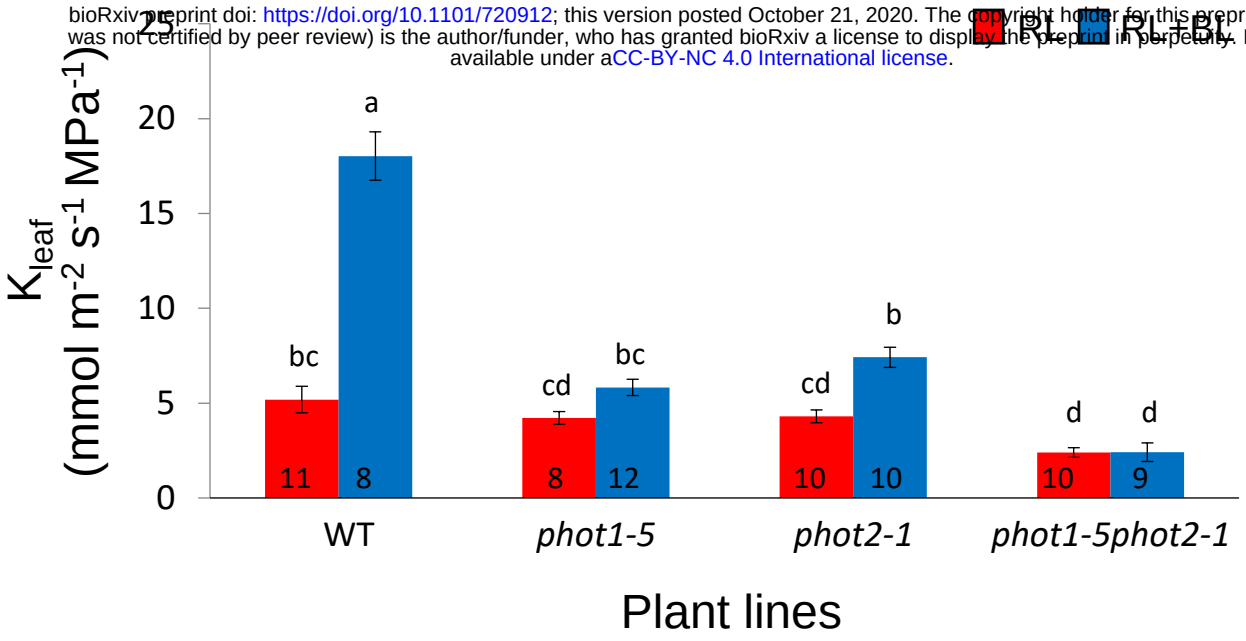

Figure 1: **The effect of blue light on K_{leaf} of PHOT receptors mutants.** K_{leaf} of fully expanded excised leaves of WT (Col-gl) and *PHOT* mutants (*phot1-5* (Col-gl), *phot2-1* (Col-gl) and a double mutant, *phot1-5 phot2-1* (Col-gl)) after illumination for 15 min immediately after dark, with RL (220 µmol m^{-2} s^{-1}), or R+BL (220 µmol m^{-2} s^{-1}, consisting of 90 % RL and 10 % BL; Materials and methods). The columns are mean values (±SE) of the indicated number of biological repeats from three independent experiments. Different letters denote significantly different values (ANOVA, *Post hoc* Tukey's test, P< 0.05) . Note the reduced response to RL+BL in the mutant lines.

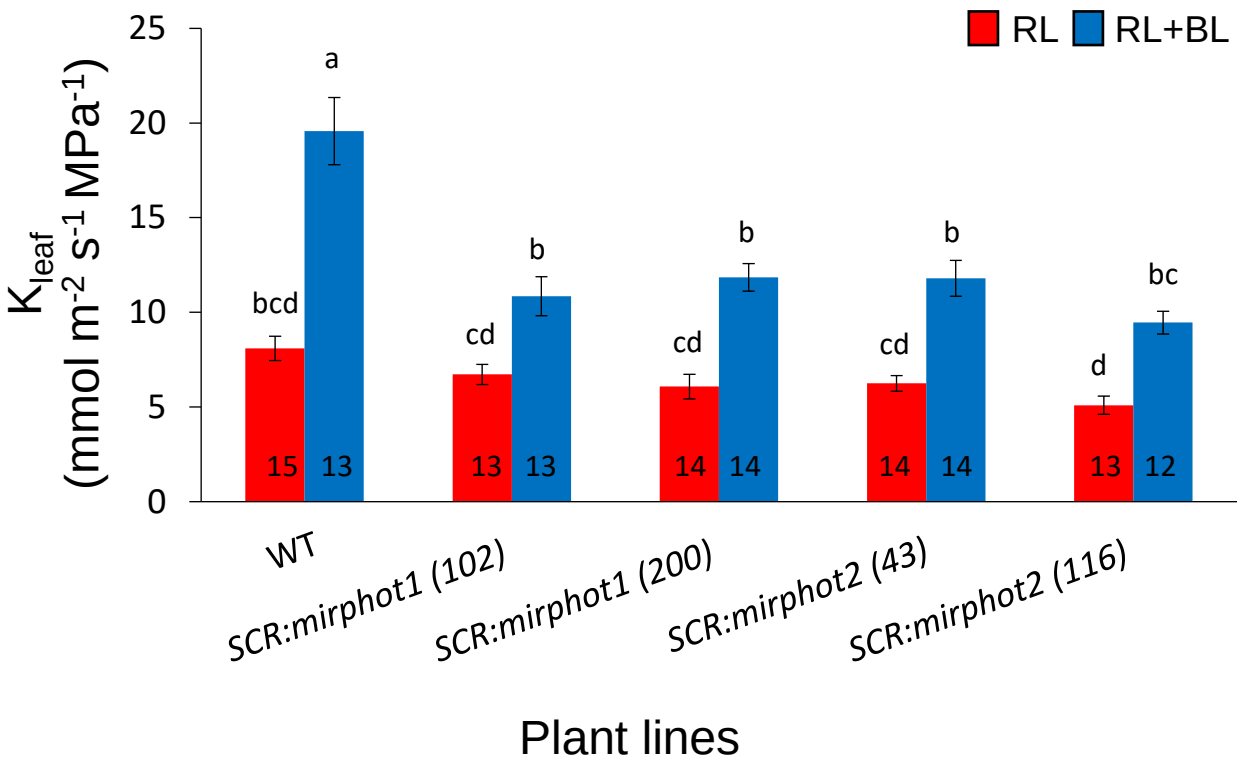

Figure 2. The effect of RL+BL on the K_{leaf} of PHOT1- and PHOT2-silenced (SCR:mir) plants, generated in WT (Col; Materials and methods). K_{leaf} was determined in fully expanded leaves of WT and *SCR:mirphot1* and *SCR:mirphot2* plants treated with RL or RL+BL (as in Fig. 1; Materials and Methods) The columns are means (± SE) of the indicated number of biological repeats from three independent experiments. Different letters denote significantly different values (ANOVA, Post hoc Tukey's test, P< 0.05).

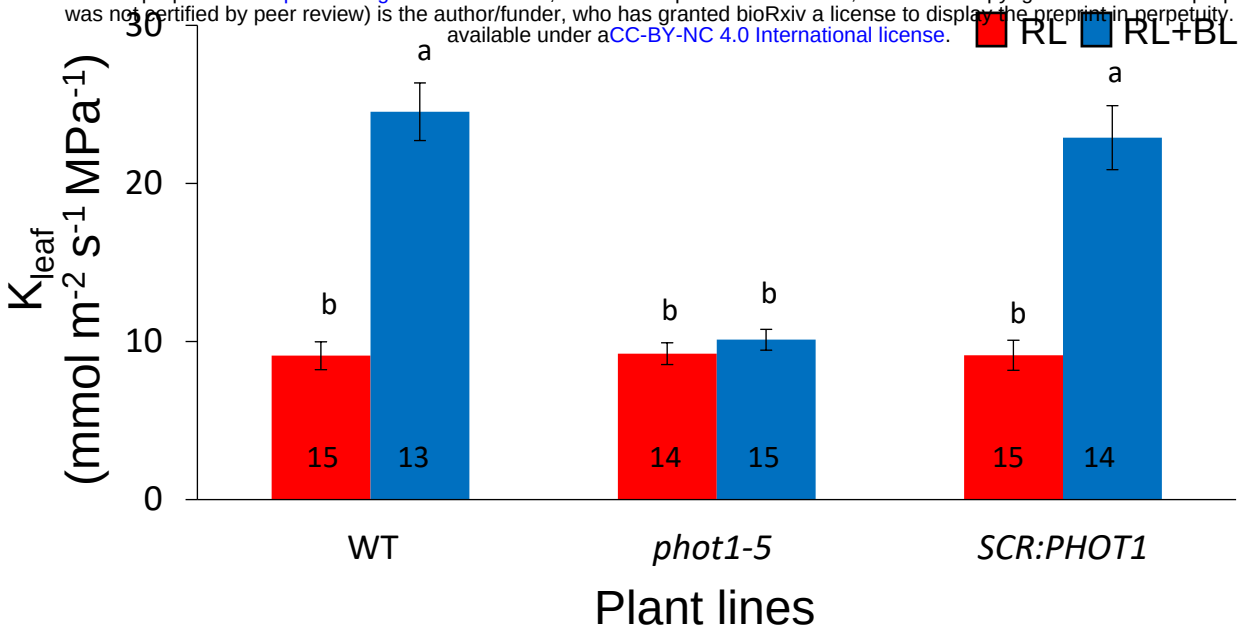

Figure 3. BSCs-directed *PHOT1* complementation of the *phot1-5* mutant restores the normal K_{leaf}. Fully expanded leaves of WT (Col-gl), *phot1-5* and *phot1-5* (Col-gl) plants complemented with *SCR:PHOT1* underwent illumination treatments as in Fig. 1. The columns are means (± SE) of the indicated number of biological repeats from three independent experiments. Different letters denote significantly different values (ANOVA,, *Post hoc* Tukey's test, P< 0.05).

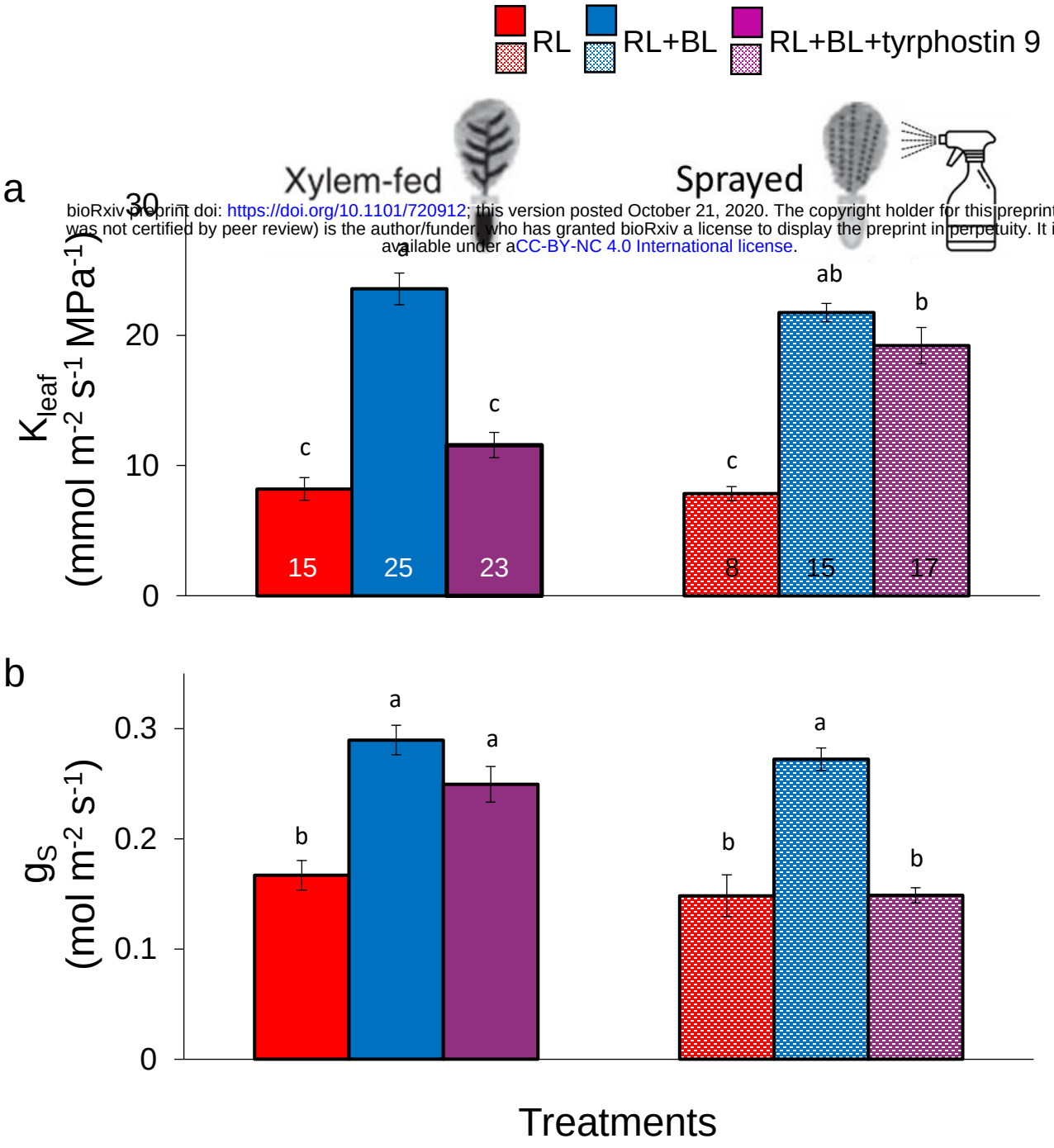

Figure 4. **Xylem-fed kinase Inhibitor tyrphostin 9 abolished the blue-light-induced K_{leaf} increase and stomatal opening.** Fully expanded leaves of WT (Col-gl) were pre-incubated (petiole deep) in AXS without or with tyrphostin 9 (10 μM) or sprayed with AXS without or with tyrphostin 9 (10 μM), and kept overnight in dark boxes. Immediately after dark, leaves were illuminated for 15 min with RL (215 μmolm^{-2} s^{-1} red) or RL+BL (215 μmol m^{-2} s^{-1}, consisting of 90 % RL and 10 % BL). **a.** K_{leaf}. **b.** Stomatal conductance (g_S). The columns are means (± SE) of the indicated number of biological repetitions, determined in three independent experimental days. Different letters denote significantly different values (ANOVA, Post hoc Tukey's test, $P < 0.05$). Note that g_S was reduced when tyrphostin 9 was sprayed but not when fed via the petiole.

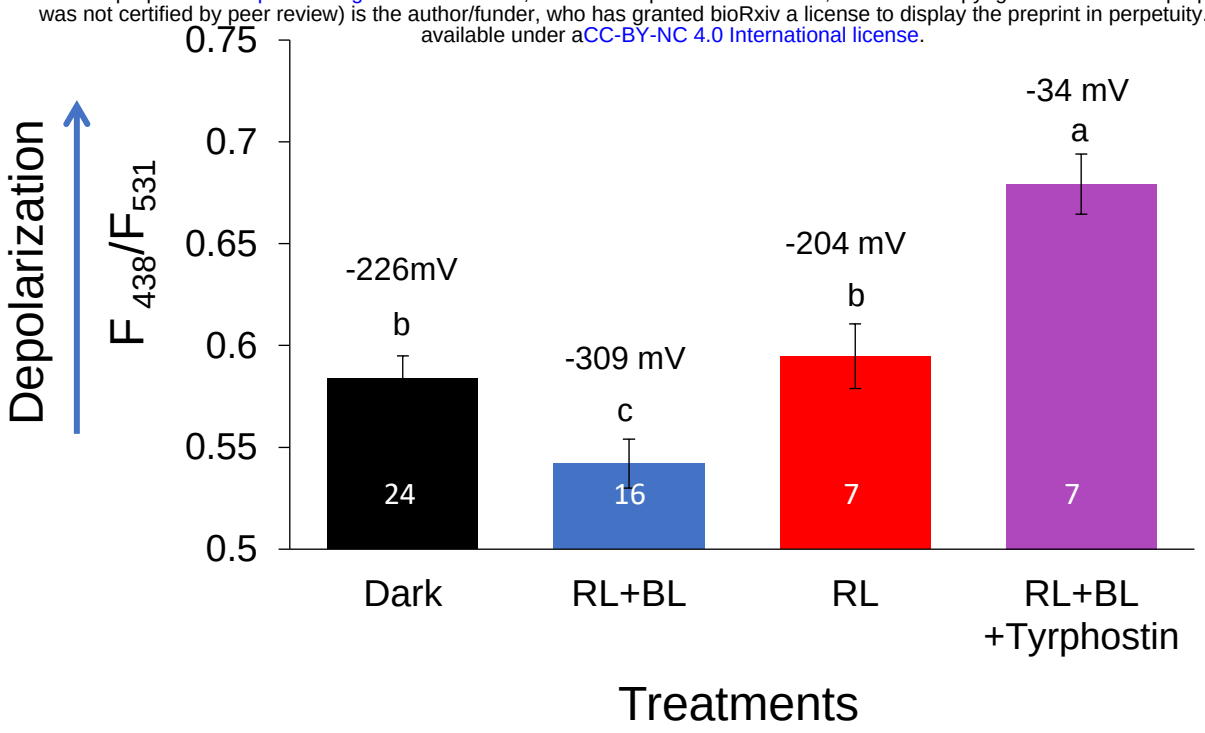

Figure 5. - Blue light (BL) hyperpolarizes the BSCs relative to red light (RL) or Dark and tyrphostin 9 depolarizes them. Membrane potential (E_M) of BSC protoplasts, without or with petiole-fed tyrphostin 9 (10 μM), determined using the dual-excitation, ratiometric fluorescent dye di-8-ANEPPS (Materials and Methods). After at least10-20 min in the dark, the cells were immediately imaged (Dark), or illuminated for an additional 5-10 minutes either with RL (220 μmol m^{-2} s^{-1}) or with RL+BL (220 μmol m^{-2} s^{-1}, including 10% BL; Materials and Methods), and then imaged. The columns are mean values of fluorescence ratio (F_{438}/F_{531}) values (±SE; n as indicated) derived from analyses of the images captured at the indicated excitation wavelengths (Materials and Methods) in three independent experiments. Numbers above the columns are the mean values of BSCs E_M, based on a calibration curve of F_{438}/F_{531} vs. E_M obtained in separate experiments using patch clamp (Materials and Methods, Suppl. Fig. S8). Different letters denote significantly different values (ANOVA, Post hoc Tukey's test, $P < 0.05$).

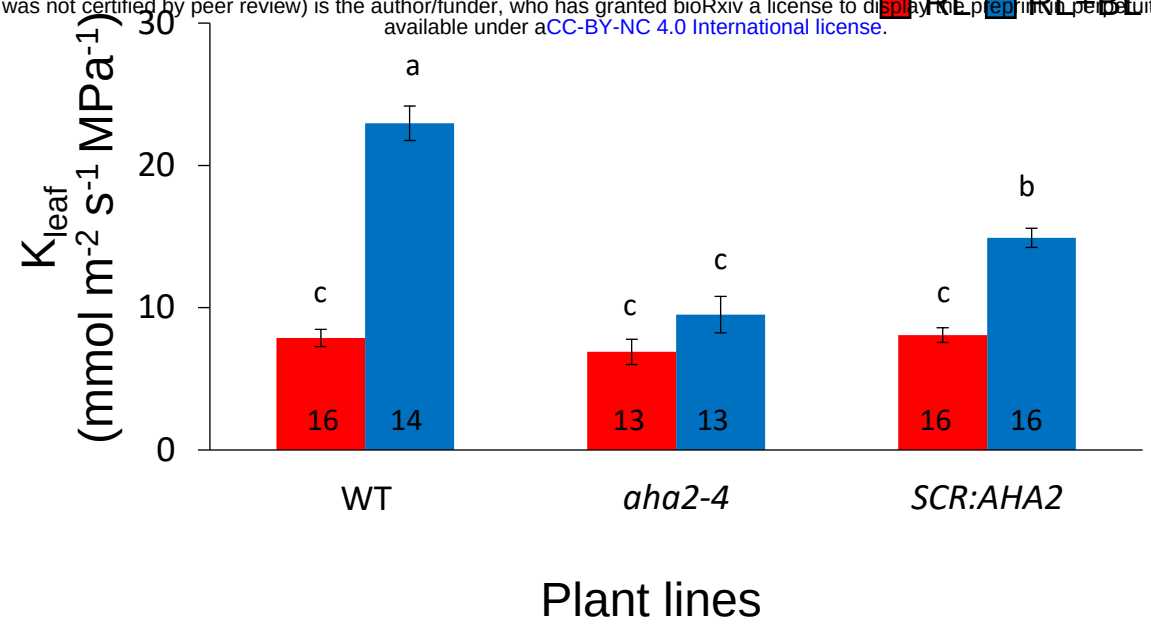

Figure 6. The BSCs H^+-ATPase, AHA2, mediates the blue-light-induced K_{leaf} increase. Fully expanded excised leaves of WT (Col0) plants, *aha2-4* mutant plants (Col0) and *aha2-4* plants complemented in their BSCs with *SCR:AHA2* were illuminated for 15 min immediately after dark, as in Fig.2. The columns are means (± SE) of the indicated number of biological repeats from three independent experiments. Different letters denote significantly different values (ANOVA, Post hoc Tukey's test, $P< 0.05$). Note the marked restoration of K_{leaf} in the *aha2* mutant plants complemented solely in their BSCs.

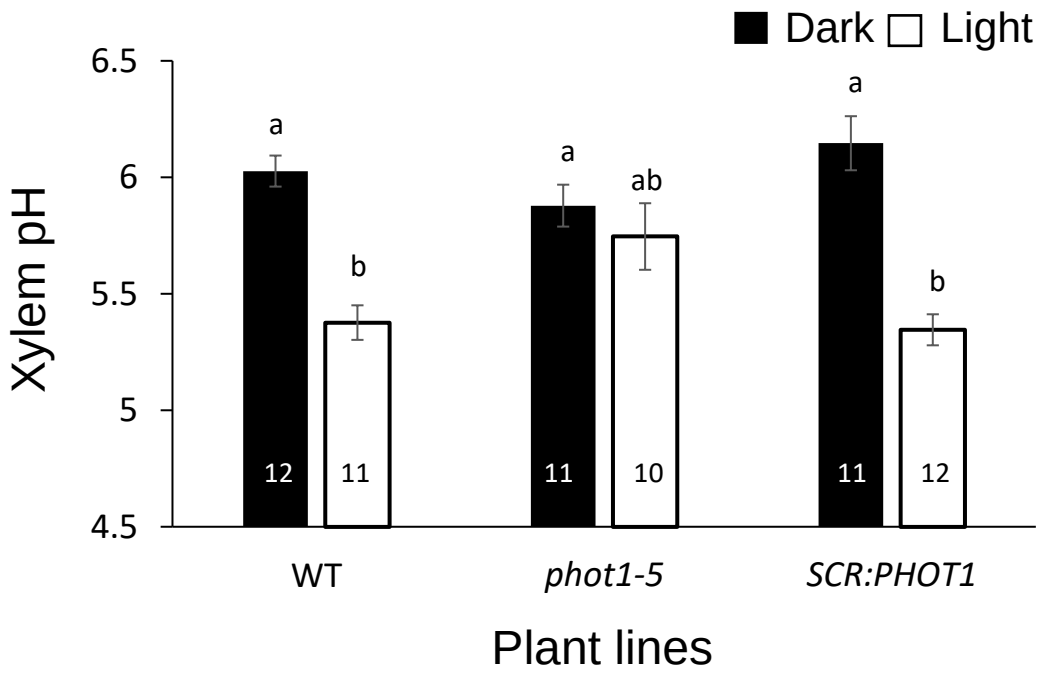

Figure 7. White light (WL) illumination for 30 minutes acidifies the xylem pH of WT plants and *SCR:PHOT1*-complemented mutants, but not in the *phot1-5* mutant. The leaves of WT (Col-gl) plants, *phot1-5* (Col-gl) mutants and the *SCR:PHOT1*-complemented *phot1-5* mutant (as in Fig. 3) were illuminated by the growth room WL (150-200 µmol m^{-2} sec^{-1}, Materials and Methods). The columns are means (±SE) of the indicated number of biological repeats from three independent experiments Different letters denote significantly different values (*Post hoc* Tukey's test, P< 0.05).

.

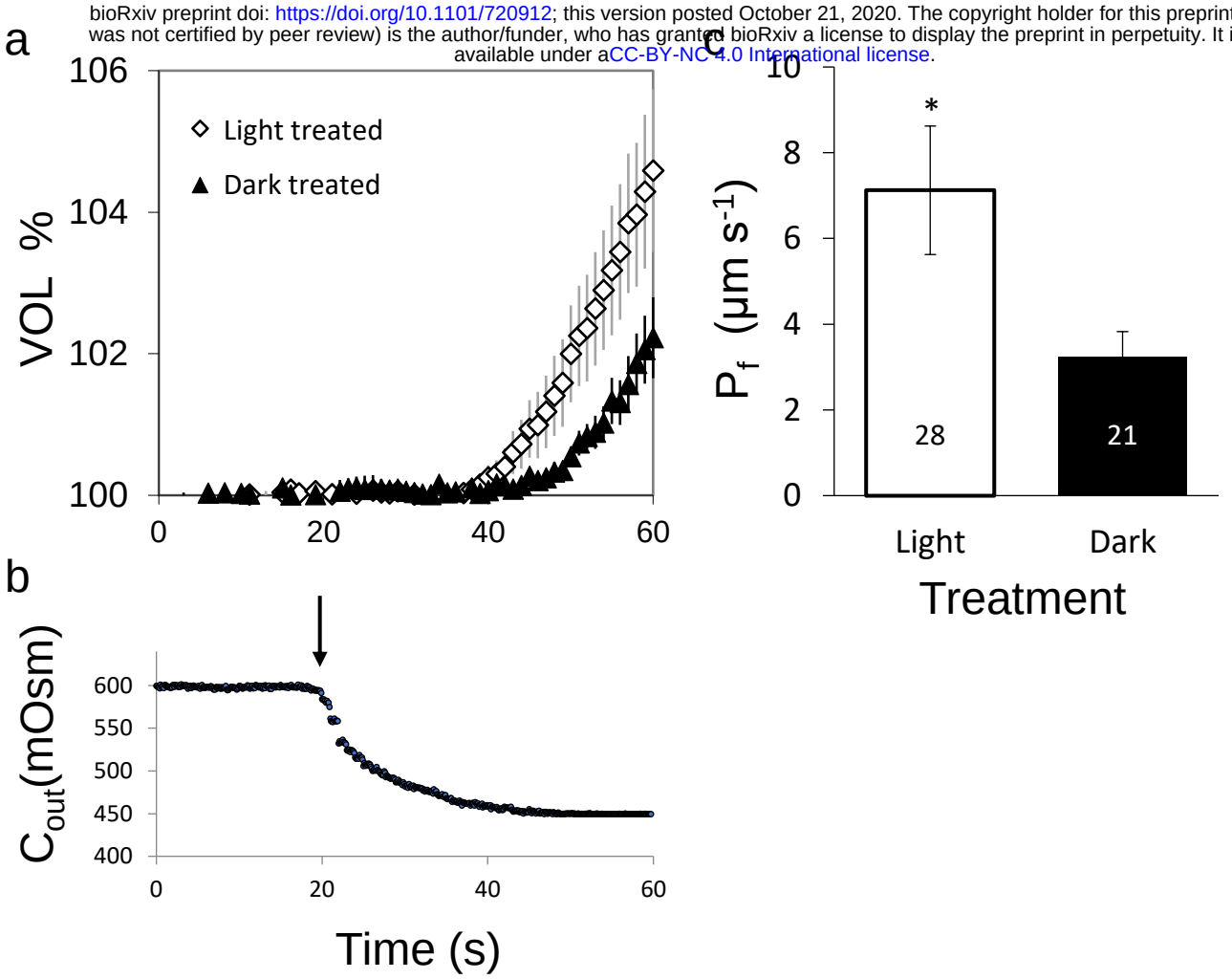

Figure 8: White light increases the BSCs membrane osmotic water permeability coefficient (P_f). **a.** A time course of swelling of bundle sheath protoplasts from *SCR:GFP* plants upon exposure to a hypotonic XPS^{db} solution under the same illumination conditions (white light or darkness) as during the light treatment preceding the assay. The bath solution was buffered to pH 5.7. The arrow indicates onset of bath flush. **b.** Time course of the osmotic concentration change in the bath (C_{out}) during the hypotonic challenge **c.** Mean (±SE) initial P_f values of the indicated number of bundle sheath protoplasts under two light regimes from three independent experiments. Columns are means (± SE) of 21-28 biological repetitions, determined in five independent experiments. The asterisk indicates a significant difference (Student's two-tailed unpaired t-test, $P < 0.05$).

Fig.8. Grunwald, GOsa et al, 2020

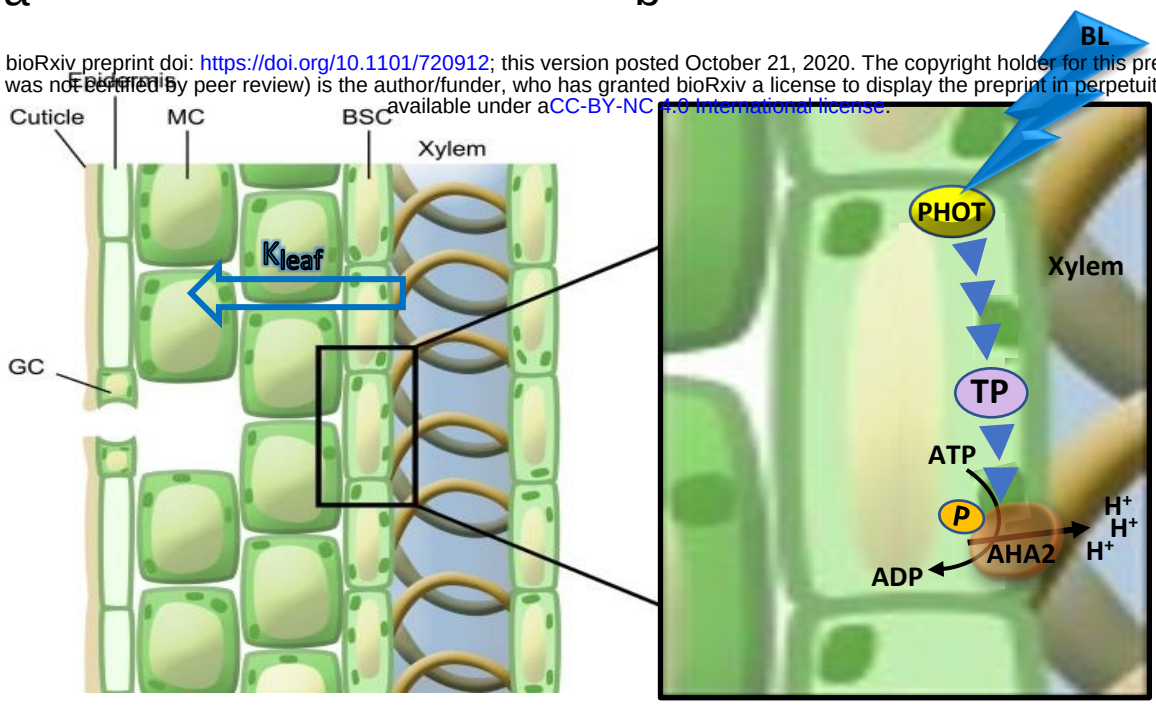

Figure 9. Proposed BSCs-autonomous BL signal transduction pathway. **a.** An artist's rendering of a leaf radial water path, from xylem to mesophyll (K_{leaf}, blue hollow arrow) via the bundle sheath cells, BSCs, which tightly envelop the xylem. GC, a stomata guard cell; MC, mesophyll cell. **b.** Blue-light (BL) signalling pathway (blue arrowheads) in a bundle sheath cell, from BL perception by the phototropin receptors (PHOT), through an intermediate tyrphostin-sensitive tyrosine phosphorylation (TP), to the ultimate AHA2 (orange circle) activation resulting in proton extrusion via the pump and xylem sap acidification, presumably, at the expense of ATP breakdown to ADP with a transient phosphorylation (P) on the pump protein, as expected from a P-type H^+-ATPase.